Journal of Crystal Growth 111 (1991) 838–842
North-Holland

Buried, ordered structures: boron in Si(111) and Si(100)

R.L. Headrick, B.E. Weir, A.F.J. Levi, D.J. Eaglesham and L.C. Feldman
AT&T Bell Laboratories, Murray Hill, New Jersey 07974, USA

Two-dimensional, metastable, ordered structures have been prepared by deposition atop unique surface reconstructions. This discovery that surface superlattice structures can be buried in crystalline semiconductors suggests possibilities for ordered doping and ordered alloy structures with new electronic properties. In this paper we summarize our recent results in forming ordered structures of boron on Si(100) and Si(111) and the preservation of these structures under subsequent Si deposition.

The first realization of preserving a surface reconstruction under a deposited layer was in the a-Si/Si(111) system where the complex 7×7 structure remained at the interface formed by clean Si(111)-7×7 and subsequent deposition of amorphous silicon (a-Si) [1]. The realization that ordered surface structures can be preserved at a buried interface suggests possibilities for new metastable materials and interesting two dimensional phenomena. In this paper we describe our recent observations of buried structures in systems consisting of ordered boron adsorbates on ⟨111⟩-oriented Si surfaces [2–4]. This atomic configuration behaves electrically as a dopant sheet of atoms with high electrical activity. Similar results have recently been reported by Akimoto et al. [5] and Tatsumi et al. [6]. In addition, we report new results of buried ordered boron layers in ⟨100⟩-oriented silicon.

Samples were prepared in a molecular beam epitaxy chamber equipped with an electron gun evaporator to deposit silicon, a quartz-crystal thickness monitor, and a Knudsen cell to deposit boron from HBO_2. Oriented ⟨111⟩ and ⟨100⟩ Si substrates were prepared by chemical growth of a thin protective oxide layer, and then transferred into the vacuum chamber. Once in the vacuum chamber, the oxide was desorbed from the sample and boron was deposited onto the surface up to a coverage of between zero and one monolayer. After cooling to room temperature, low energy electron diffraction (LEED) and Auger electron spectroscopy measurements were performed. Finally, the surface was capped with silicon at various temperatures. All other measurements, including grazing incidence X-ray diffraction, ion scattering/channeling, transmission electron microscopy, and low temperature ($T = 4.2$ K) Hall effect measurements were done after removing the capped samples from the vacuum system.

Glancing angle X-ray diffraction, scanning tunneling microscopy and first-principles theoretical calculations have established the structure of the Si(111)–B-$\sqrt{3} \times \sqrt{3}$ surface as boron in a subsurface site, arranged in a $\sqrt{3} \times \sqrt{3}$ configuration [3,7]. Fig. 1 shows this site and compared it to the more common $\sqrt{3} \times \sqrt{3}$ configuration (T_4 site) for Ga and other adsorbates. The stability of boron in the subsurface site relative to the T_4 adatom site is related to relief of subsurface strain by the mechanism of substituting a smaller boron atom for silicon [3].

The fact that this ordered structure is maintained upon room temperature deposition of a-Si is shown in fig. 2, which compares the glancing angle X-ray diffraction of both the Ga and B structures. Retention of the strong third order diffraction intensity in the boron case clearly indicates that the boron retains its $\sqrt{3} \times \sqrt{3}$ structure while Ga becomes disordered. Detailed Auger measurements show that the Ga surface segregates during Si deposition at room temperature, while

0022-0248/91/$03.50

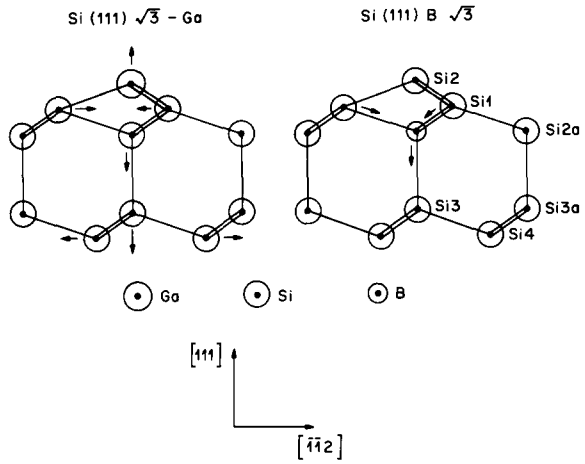

Fig. 1. Model of the Si(111)–Ga-$\sqrt{3}$ structure and proposed structure for Si(111)–B-$\sqrt{3}$ (right). Arrows indicate the direction of displacements from the ideal tetrahedrally bonded configuration.

boron remains in a buried, ordered in configuration. Such segregation behavior is consistent with the buried site for boron and an atop site for Ga.

A desired configuration would correspond to epitaxial Si atop the ordered boron configuration.

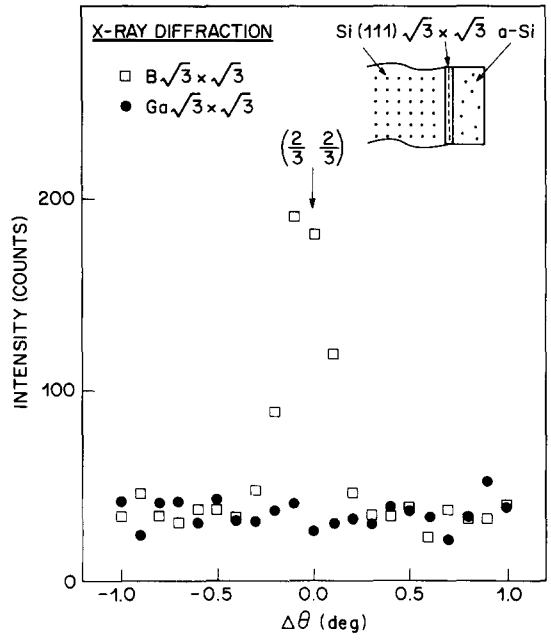

Fig. 2. Rocking scan through the $(\frac{2}{3}\frac{2}{3})$ surface X-ray diffraction rod for buried boron and gallium surface structures on Si(111).

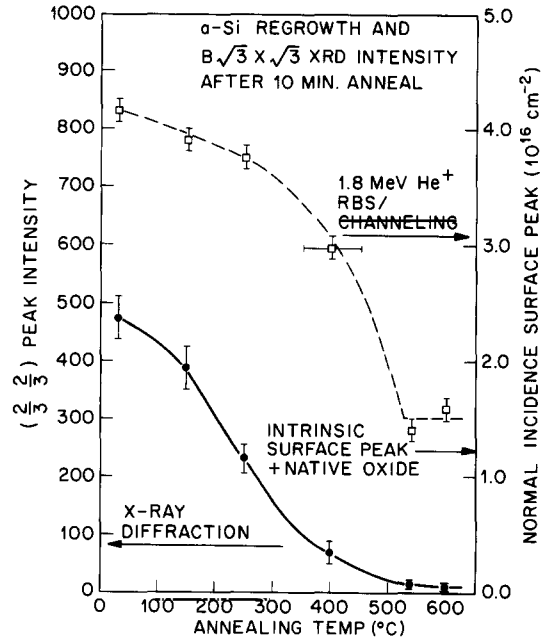

Fig. 3. Dependence of the $(\frac{2}{3}\frac{2}{3})$ surface X-ray diffraction integrated intensity as a function of annealing temperature for the boron $\sqrt{3} \times \sqrt{3}$ surface structure originally covered with a-Si (~ 100 Å) (filled in circles). Also shown is the temperature dependence of normal incidence channeling for the Si overlayer indicating complete epitaxial regrowth at ~ 500 ° C.

Two possible methods of achieving this structure are: (1) epitaxial regrowth of the amorphous layer or (2) high temperature deposition of Si for epitaxial growth. Neither method works ideally in the Si(111)–B-$\sqrt{3} \times \sqrt{3}$ case. Fig. 3 shows the decrease of the $\sqrt{3} \times \sqrt{3}$ intensity with regrowth temperature. Epitaxy in the Si overgrown layer is indicated by channeling measurements which indicate crystallization with increasing temperature. The X-ray intensity corresponding to the $\sqrt{3}$ structure deteriorates with regrowth, indicating a disordering of the boron structure as epitaxial regrowth occurs. High temperature (~ 550 ° C) deposition of Si also results in boron disordering and surface segregation, indicating that the metastable structure associated with the ordered, δ-layer is not stable at Si epitaxy temperatures. A separate series of measurements indicated that the lowest temperature for Si(111) epitaxy is ~ 400 ° C, however even at this low temperature some boron disordering occurs.

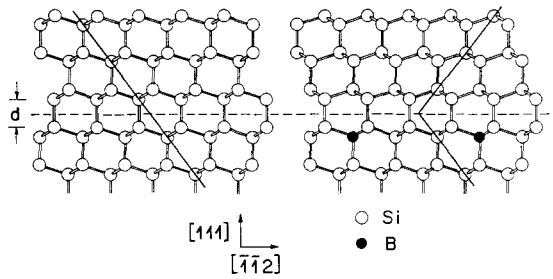

Fig. 4. Ball and stick models for the film orientation and interface structure for 0 (left) and 0.33 ML (right) boron coverages. The $\sqrt{3} \times \sqrt{3}$ reconstruction of the interface is introduced because boron occupies substitutional sites, occupying every third site in a single monolayer at the interface.

An interesting phenomenon is observed for Si epitaxial growth on the B-$\sqrt{3}$ structure at low temperatures. Evidently the initial layers of Si epitaxial growth are strongly influenced by the Si–B interaction, giving rise to a 180° rotated configuration of the grown layer of Si (fig. 4). The existence of this layer is most strikingly demonstrated in fig. 5 which shows glancing X-ray diffraction intensity from a 350 Å Si layer grown at ~ 400 °C on Si(111)–B-$\sqrt{3}$ at and then further annealed.

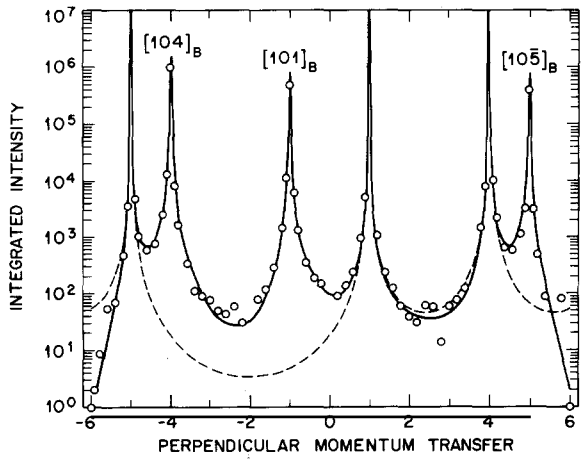

Fig. 5. (10) rodscan for a 350 Å rotated Si film on Si(111). A four-circle diffractometer and Cu Kα radiation was used for the measurement. The diffraction profiles are indexed relative to a hexagonal unit cell appropriate for the Si(111) surface with in-plane lattice parameters $a = b = 3.84$ Å and out-of-plane lattice parameter $c = 9.41$ Å. The hexagonal indices are derived from cubic indices by $[10l]_{hex} \equiv \frac{1}{3}[\bar{4}22]_{cub} + \frac{1}{3}l[111]_{cub}$. Rotated reflections are indexed by replacing l by $-l$. Structure factors at $-l$ were obtained by the symmetry relation $[10\bar{l}] = [01l]$. The dashed line is the calculated intensity from a "bulk-like" structure, the full line is for a 350 Å rotated film atop a bulk crystal.

The X-ray crystal truncation rod method using integer h and k but continuous l, originally developed for determination of surface structures, is used to identify this thin film structure. A total of 66 data points in the form of structure factors $F_{hk}(l)$ were obtained by numerical integration of rocking curves and corrected for the Lorentz factor ($\sin 2\theta$) and active area ($\sin 2\theta$). We compared ($10l$) crystal truncation rod data for a 350 Å silicon film grown at 400 °C and annealed at 1000 °C for 2 h to structure factors calculated in the kinematic approximation (fig. 5). The film is rotated 180° with respect to the substrate about the normal (111) axis, forming a single twin at the interface. The dashed line is the square of $F_s(l)$, the structure factor $F_{10}(l)$ for the semi-infinite silicon substrate with double-layer termination. There are three prominent peaks that do not correspond to the substrate. The new peaks are accounted for by adding the 350 Å thick rotated film into the calculated structure factor. The solid line shows the results of a calculation with a 233 monolayer, rotated layer. The optimum interface separation was $d = 2.35 \pm 0.09$ Å, i.e. the same as the bulk layer spacing. This shows that the simple twin stacking sequence is the correct interface structure. Transmission electron microscopy confirms this assignment showing that the layer is at least 90% crystallographically pure [8].

We have recently reported a new boron-induced (2×1) surface reconstruction at 1/2 monolayer boron coverage on ⟨100⟩ oriented silicon [9]. To our knowledge this reconstruction has not been reported previously, presumably because of the difficulty in distinguishing the Si(100)-(2×1) clean surface from the (2×1) boron structure. In sharp contrast to the results on ⟨111⟩-oriented silicon discussed above, we find that this reconstruction can be preserved within high-quality, *crystalline* silicon by low-temperature epitaxial overgrowth at ≈ 300 °C. For boron coverages at and below the completion of the (2×1) surface phase and silicon overlayer growth temperatures of 300 °C and above, 100% of the boron is electrically active.

Fig. 6 shows grazing incidence X-ray diffraction azimuthal scans through $(\frac{3}{2}0)$ surface reflections for two ordered interfaces. The open squares are for a 100 Å cap grown at room temperature, and the filled circles are for a 100 Å cap grown at 300 °C. The boron coverage is 1/2 monolayer in both cases. Comparison of the data demonstrates that the reconstruction capped at 30 °C gives a factor of two smaller integrated intensity in the diffraction signal than the reconstruction capped at room temperature. Boron segregation studies using Auger electron spectroscopy for films grown at 300 °C reveal a broadening of the ideal monolayer distribution by ≈ 5 Å. This is consistent with the observation that ≈ 50% of the boron remains in the ordered layer.

Cross-sectional transmission electron microscopy and ion channeling studies show that the 100

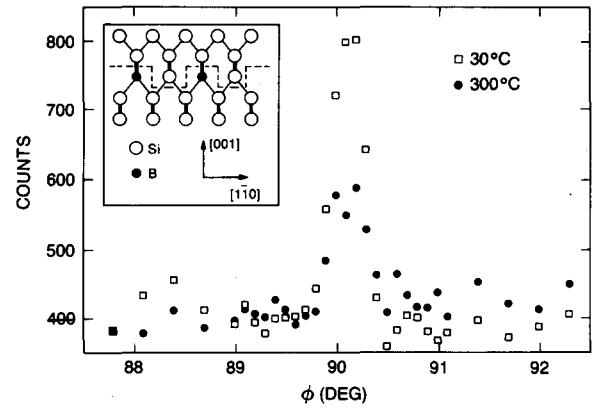

Fig. 6. Comparison of grazing incidence X-ray diffraction azimuthal scans through the $(\frac{3}{2}0)$ diffraction spot for Si(100)-(2 × 1) boron buried structures capped by growth at room temperature, and at ≈ 300 °C. The boron coverage was 1/2 monolayer in both cases and the silicon growth rate was 0.1 Å/s. The inset shows a proposed model of the (2 × 1) structure.

Table 1
4.2 K Hall effect results for Si(111)/a-Si interface reconstructions

Reconstruction		a-Si thickness (Å)	T_{anneal} (°C)	Boron coverage (10^{14} cm^{-2})		Carrier density (10^{14} cm^{-2})	Mobility (cm^2 V^{-1} s^{-1})
Initial	Final			SIMS	NRA		
$\sqrt{3}$	$\sqrt{3}$	100	90	3.4	3.5	2.2	36.6
$\sqrt{3}$	$\sqrt{3}$	60	90	2.6	2.7	1.7	30.5
$\sqrt{3}$	$\sqrt{3}$	50	90	3.1	3.4	1.8	25.9
$\sqrt{3}$	3D	100	700	3.4	3.5	3.2	47.9
$\sqrt{3}$	Oxide	0	90	3.1	3.4	0	–
$\sqrt{3}$	3D	60	500	2.6	2.7	2.4	31.9
7×7	7×7	50	90	0.1	–	0	–

Table 2

Film thickness (Å)	T_{growth} (°C)	T_{anneal} (°C)	Anneal time (min)	Boron coverage (ML)	Carrier density (ML)	Mobility (cm^2 V^{-1} s^{-1})
100	300	90	20	0.44	0.45	21
100	30	90	20	0.50	0.24	1
100	30	90	20	0.50	0.18	3
100	30	90 [a)]	≈ 3000	0.47	0.12	19
100	30	400	1	0.11	0.07	14
100	30	400	1	0.31	0.18	21
100	30	400	1	0.51	0.32	16
100	30	400	1	0.83	0.33	18
100	30	400	60	0.50	0.35	17

[a)] Boiled in distilled water.

Å thick films grown at 300 °C are high quality crystalline silicon indistinguishable from bulk silicon, while room temperature growth results in an amorphous layer. Channeling measurements (in ⟨100⟩ normal incidence and ⟨111⟩ off-normal incidence) using the $^{11}B(p, \alpha)^{8}Be$ nuclear reaction to detect boron, show a reduced yield compared to random incidence after silicon overgrowth at 300 °C, indicating that boron occupies a substitutional site buried within crystalline material.

We now discuss the electrical activity of boron doped silicon structures prepared via the (2×1) and $(\sqrt{3} \times \sqrt{3})$ reconstruction. Tables 1 and 2 gives carrier densities and mobilities from low temperature ($T = 4.2$ K) Hall effect measurements for silicon overlayers grown at 30 and 300 °C, and annealed at various temperatures. There was no carrier freeze-out and no significant magnetoresistance for any of the samples measured. Units of monolayers are used for clarity, where one monolayer is defined as 6.8×10^{14} cm^{-2} for Si(100) and 7.8×10^{14} cm^{-2} for Si(111). The optimum conditions for producing electrically active ordered doping layers in epitaxial silicon (100) are a boron coverage of 1/2 monolayer and a silicon growth temperature of 300 °C. Under these conditions 100% electrical activity and a mobility of 21 cm^2 V^{-1} s^{-1} are obtained. This mobility is comparable to that obtained for very high boron concentrations in bulk silicon [10].

Conclusions: We have shown that two-dimensional ordered layers or boron can be preserved at the Si(111) and Si(100) surfaces. In the Si(100) case epitaxial Si can be grown atop the ordered structure. All systems show a high p-type electrical activity, between 50% and 100% electrically active.

References

[1] J.M. Gibson, H.-J. Gossmann, J.C. Bean, R.T. Tung and L.C. Feldman, Phys. Rev. Letters 56 (1986) 355; H.-J. Gossmann, L.C. Feldman and W.M. Gibson, Phys. Rev. Letters 53 (1984) 294; Surface Sci. 155 (1985) 413; H.-J. Gossmann and L.C. Feldman, Phys. Rev. B32 (1985) 6.

[2] R.L. Headrick, L.C. Feldman and I.K. Robinson, Appl. Phys. Letters 55 (1989) 442.

[3] R.L. Headrick, I.K. Robinson, E. Vlieg and L.C. Feldman, Phys. Rev. Letters 63 (1989) 1253.

[4] R.L. Headrick, A.F.J. Levi, H. Luftman, J. Kovalchick and L.C. Feldman, Phys. Rev. B, to be published.

[5] K. Akimoto, J. Mizuki, I. Hirosawa, T. Tatsumi, H. Hirayama, N. Aizaki and J. Matsui, in: Extended Abstracts 19th Conf. on Solid State Devices and Materials (Business Center for Academic Societies, Tokyo, 1987) p. 463.

[6] T. Tatsumi, I. Hirosawa, T. Nino, H. Hirayama and J. Mizuki, Appl. Phys. Letters. 57 (1990) 73.

[7] P. Bedrossian, R.D. Meade, K. Mortensen, D.M. Chen and J.A. Golovchenko, Phys. Rev. Letters 63 (1989) 1257; I.-W. Lyo, E. Kaxiras and Ph. Avouris, Phys. Rev. Letters 63 (1989) 1261.

[8] R.L. Headrick, B.E. Weir, D.J. Eaglesham and L.C. Feldman, Phys. Rev. Letters 65 (1990) 1128.

[9] R.L. Headrick, b.E. Weir, A.F.J. Levi, D.J. Eaglesham and L.C. Feldman, Appl. Phys. Letters, to be published.

[10] G. Masetti, M. Severi and S. Solmi, IEEE Trans. Electron Devices ED-30 (1983) 764.